HEFAT2014
10th International Conference on Heat Transfer, Fluid Mechanics and Thermodynamics
14 – 16 July 2014
Orlando, Florida

FALLING FILM EVAPORATIVE HEAT TRANSFER ON CNT COMPOSITE COATINGS

Won-seok Choi, Seok-min Kang, Eun-seok Wang, Min-soo kim and Chan-woo Park*
*Author for correspondence
Division of Mechanical Design Engineering
Chonbuk National University,
Jeonju, Jeonbuk, 561-756
Korea,
E-mail: cw-park@jbnu.ac.kr

ABSTRACT

This study aims to enhance falling film type evaporation heat transfer on metal surfaces by coating with multi-walled carbon nanotubes (MWCNTs). In order to do this, multi-walled carbon nanotube/Copper (MWCNT/Cu) composite powders fabricated and composites are sprayed on the surface of Copper plates and are sintered. The falling type evaporation heat transfer tests were performed under working conditions of absorption chiller for water(Pressure: 4 mm Hg). Then the heat transfer tests were performed with various contents of MWCNT coated specimens and falling flow rates of refrigerants. Based on the results, it can be inferred that evaporation heat transfer was enhanced due to the porous structure of the surface coating and the excellent heat transfer characteristics of the MWCNTs.

INTRODUCTION

Recently, due to the growing global interest in environmental protection and interest in the reduction of energy consumption brought about by the rising international oil prices, low-carbon green technology development has become a very important research direction. Especially, due to the large industrial and economic impact of the reduction of power consumption of energy devices, the efficiency of powder plant boilers, evaporators of refrigeration/air conditioning systems, industrial and household heat exchangers have to be increased. In heat exchangers such as these, where a lot of boiling heat transfer occurs, improvement of boiling heat transfer becomes very important when considering world wide environmental protection (Lee & Jung, 2009).

In 1991, carbon nanotubes (CNTs) were manufactured by Dr. Ijima using an electric discharge method from graphite sheets. They were formed with rounded curled tubular features having diameters of only tens of nanometers. They have a cylindrically shaped molecular structure with the carbon atoms arranged in a hexagonal honeycomb fashion. Due to the unique molecular structure, CNTs exhibit excellent mechanical, electrical, thermal, and optical properties and have attracted considerable attention for future applications (Ajayan, 1999; Dresselhaus, Dresselhaus, & Avouris, 2001). The thermal conductivity of CNT is twice that of diamond, its electrical conductivity is higher than that of copper, it is 100 times stronger than steel at the same thickness, and it is light in weight. This study aims to enhance falling film evaporation heat transfer on metal surfaces by coating them with multi-walled carbon nanotubes (MWCNTs). In order to do this, multi-walled carbon nanotube/copper (MWCNT/Cu) composite powders fabricated by attrition ball milling are sprayed on the surface of coopper plate specimens and are sintered. Then the falling film evaporation heat transfer performance of the coated specimens was investigated.

NOMENCLATURE

A	[cm^2]	*Area*
H	[W/m^2K]	Heat transfer coefficient
I	[A]	Current
k	[W/mK]	Thermal conductivity
Q	[W]	Heat transfer rate
T	[℃]	Temperature
V	[V]	Volt

Subscripts

sat	Saturation
wall	Wall/surface

EXTERNAL BOUNDARY CONDITIONS

The fabrication of MWCNT/Cu composite powder was done by milling MWCNT and Cu powder in an attrition ball mill for 4 h with 5-mm zirconia balls and an argon environment. A prepared 2 Wt.% polyvinyl alcohol (PVA) solution was sprayed on the Cu plate substrates after which pure Cu powder was sprayed using an electrostatic spray. On top of the sprayed Cu powder, the spraying of PVA was repeated and then the MWCNT/Cu composite powder was sprayed with the

electrostatic spray. Fig. 1 illustrates the fabrication process of the specimens. After the spraying of the powders, the coated plates were placed inside an electric furnace. The temperature was raised from room temperature to 350°C at the rate of 20°C min-1 and held for 10 minutes to remove the PVA. The temperature was further raised up to 600°C and held for one hour in a mixed gas (10% hydrogen, 90% nitrogen) environment for reduction and sintering. Then the furnace was cooled down to room temperature.

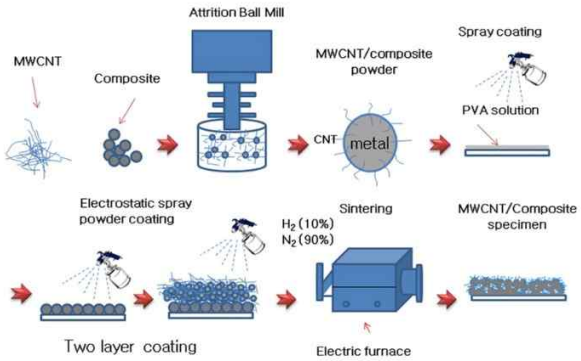

Figure 1 Schematic of the coating fabrication process

NUMERICAL METHOD

Fig. 2 and 3 illustrates the test section and the heat transfer test set-up, respectively. Each of the fabricated plate specimens was attached on the test section. The test section was then installed in the test chamber. The chamber was vacuumed and refrigerant was charged into the chamber. The evaporation heat transfer test was done by spraying liquid refrigerant to the surface of the specimen through the nozzle and by heating the specimen surface using the heater installed in the test section. In order to maintain the temperature of the refrigerant in the chamber, coils with for cooling water and cartridge heater were installed. Also, the external part of the chamber was covered with thermal insulator to prevent or minimize heat loss or heat gain. Each specimen was placed in a horizontal position perpendicular to the film evaporation heat transfer direction. The flow of the refrigerant being sprayed on the surface was set to 5 cc, 10 cc, and 20 cc. Two kinds of the refrigerants(Pure water and R134a) are used.

The details of the test section are shown in Fig. 2. It has an electric heater and a Cu block measuring 10 x 10 x 3 mm. The Cu block was attached on top of the heater. Two T-type thermocouples are embedded at the middle part 1.5 mm below of the surface of the block to measure the block's temperature. The heat flux was controlled by controlling the DC power that was supplied to the heater. All the pressure and temperature readings were gathered using an Agilent 34972A data acquisition unit and the data were recorded in a computer using a LabVIEW program.

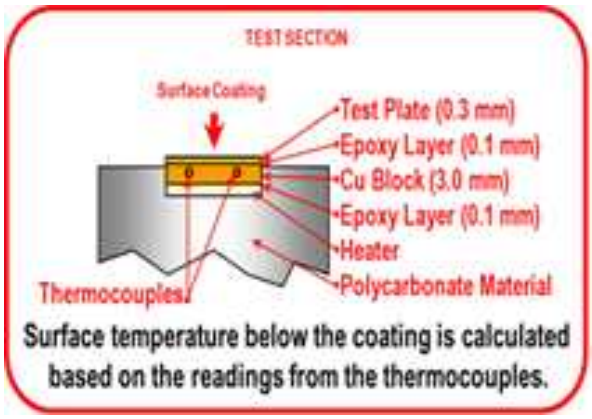

Figure 2 Test Section

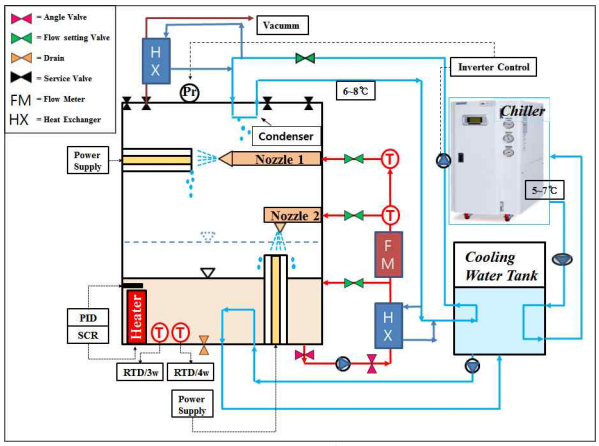

Figure 3 Heat transfer test set-up

PROCESSING OF RESULTS

The heat transfer rate along the specimen is estimated from Eq. (1), where Q, V, and I are the heat transfer rate that is equal to the heater power input, voltage of the power supply, and current of the power supply, respectively. The local heat transfer coefficient, h, at the substrate plate surface was calculated using Eq. (2), where A, Twall and Tsat are the projected area of the coating, surface temperature of the substrate plate and the temperature of the refrigerant, respectively.

$$Q = VI \tag{1}$$

$$h = \frac{Q}{A(T_{wall} - T_{sat})} \tag{2}$$

TRENDS AND RESULTS

Fig. 4 shows the FE-SEM image of the MWCNTs before ball milling. As shown, the MWCNTs have long strand-like shape. Fig. 5 shoe the FE-SEM image of the composite 10 vol.% MWCNT/Cu powder after ball milling for 4 h using zirconia balls. The long shape of the intertwined MWCNT in Fig. 4 can be confirmed in Fig. 5. However, due to the ball milling, the

MWCNTs were cut short. This improved the dispersion and the embedding of the MWCNTs in the Cu particles.

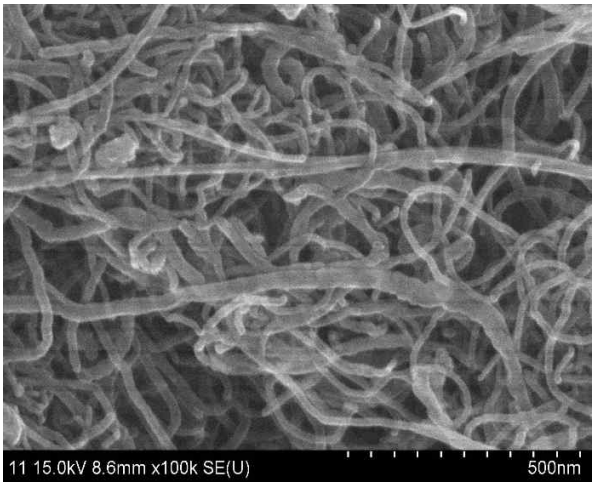

Figure 4 FE-SEM micrograph of the MWCNT

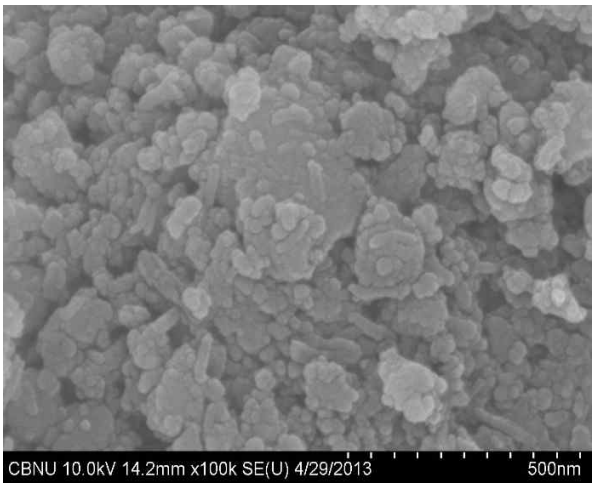

Figure 5 FE-SEM micrograph of 10 vol.% MWCNT/Cu

Fig. 6 shows the FE-SEM image of the surface of the sintered coating fabricated from 20 vol.% MWCNT/Cu composite powder that was ball-milled for 1 h. Fig. 7 shows the coating made from the 20 vol.% MWCNT/Cu composite powder that was ball-milled for 4 h. The coatings were sintered at 600°C for 1 hr. The relatively long geometry of the MWCNTs can be observed. Also, we observed that with the increase of ball milling time the MWCNT were finely cut and blended were with the Cu powder particles

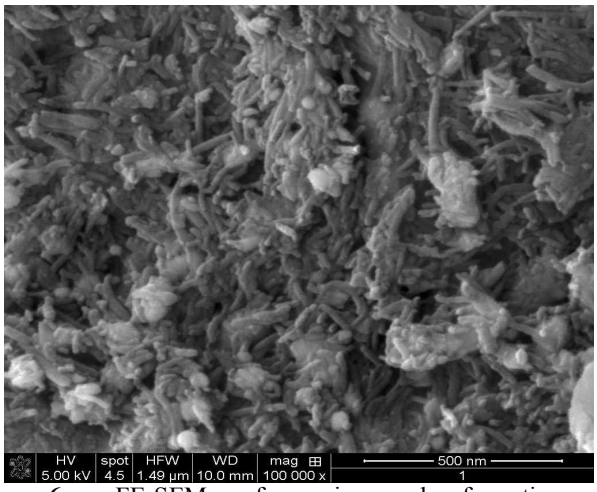

Figure 6 FE-SEM surface micrograph of coating made from 20 vol.% MWCNT/Cu powder ball-milled for 1 h

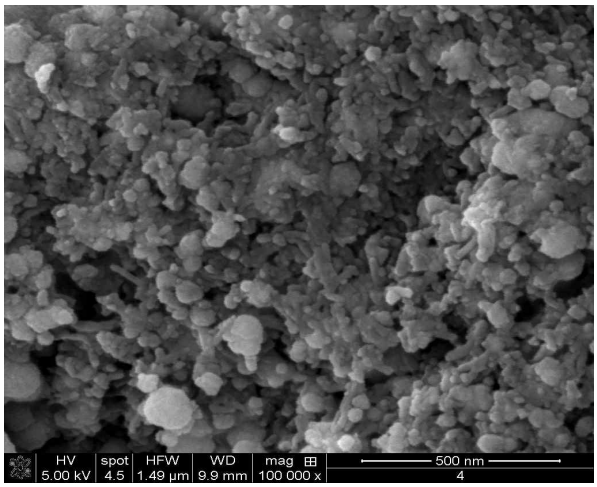

Figure 1 FE-SEM surface micrograph of coating made from 20 vol.% MWCNT/Cu powder ball-milled for 4 h

Fig. 8 and Fig. 9 show the falling film evaporation heat transfer test results at different refrigerant flow rates. Fig. 8 shows the variation of the heat flux. It can be seen that heat flux values of the MWCNT/Cu coatings were higher that those of the bare Cu plate. Also, the heat flux increased with the increase of the flowrate. The increase of ΔT indicates the increase of superheat. Fig. 9 shows the variation of the falling film evaporation heat transfer coefficients. As mentioned in section 3.2, the ball milling of the MWCNT and the Cu powder cut the MWCNT into shorter strands and improved the dispersion of the MWCNT in the Cu powder matrix. A consequence of this was increased ability of the MWCNT/Cu composite coating for heat transfer enhancement as can be seen from the results. Moreover, it is known the high thermal conductivity of the MWCNT is only observed along its access. This means that this unique characteristic in only single directional. But, through ball milling, the cutting and dispersion of the MWCNTs in the Cu matrix rendered the resulting composite an improved high thermal conductivity that is multi-directional.

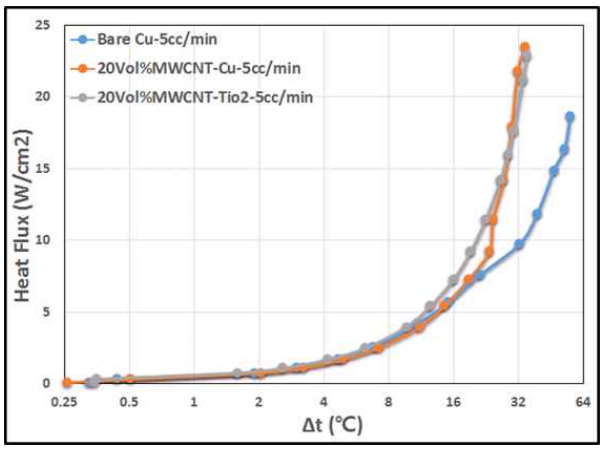

Figure 8 Variation of falling film evaporation heat flux

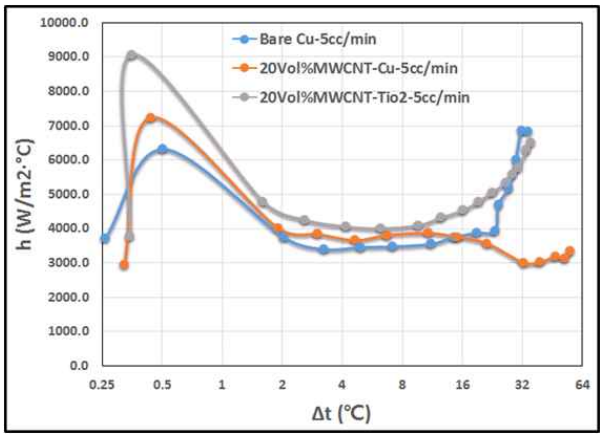

Figure 9 Variation of falling film evaporation heat transfer coefficient

CONDITIONS WITH THERMAL INTERFACIAL RESISTANCE

When thermal interfacial resistance, either internally between heat generating and cooling layers; or externally between the composite heat-generating bi-material component and external cooling components are no longer negligible, the thermal performance increase of an embedded cooling layer scheme is reduced. It was found that at small dimensional scales in the order of 10 mm or less for $\mathcal{Z}$, interfacial resistance values of 0.0001 m^2K/W reduced $E_{\%,eff}$ by 20%. For cases where critical layer conditions are reached, the maximum thermal performance equation as is given in equation (6) need to be adjusted to incorporate the influences of thermal interfacial resistances, R_{int} and R_{ext}, thermal conductivities, k_M and k_C, and dimension $\mathcal{Z}$. When critical layering conditions are however not reaches, additional geometric influences are required to determine $E_{\%,eff}$. Due to length restrictions the description of these dependencies fall beyond the scope of this paper.

CONCLUSION

1. The MWCNTs, which were long and entangled before ball milling, became short and were embedded into the Cu powder particles after ball milling.

2. Based on the results, in can be inferred that evaporation heat transfer was enhanced due to the porous structure of the surface coating where many bubbles were generated and due to the excellent heat transfer characteristics of the MWCNTs. The coatings made from sintered ball-milled MWCNT/Cu composite powder had improved heat transfer characteristics.

REFERENCES

[1] Y. H. Lee, D. S. Jung, Boilling Heat Transfer Cofficients of Nanofluids Using Carbon Nanotubes, Journal of the Korean Solar Energy Society Vol.29, No.5, 2009. pp.35-44

[2] Lee, J. W., L ee, D. Y. and Kang, B. H., 2003, An experimental study on the effects of porous layer treatment on evaporative cooling of an inclined surface, Korean Journal of Air-Conditioning and Refrigeration Engineering, Vol. 17, No. 1, pp. 25-32.

[3] Cheng-Chieh Hsieh, Shi-Chune Yao, 2005, Evaporative heat transfer characteristics of a water spray on micro-structured silicon surfaces, International Journal of Heat and Mass Transfer, Vol. 49, pp. 962–974.

[4] Kim. K. h, Kang. H. B, LEE. D. Y., 2006, An Experimental Study on the effects of Contact Angle on a Falling Liquid Film.

[5] Elizaveta Ya. Gatapova. Andrey A. Semenov. Dmitry V. Zaitsev. Oleg A. Kabov. 2013, Evaporation of a sessile water drop on a heated surface withcontrolled wettability.

[6] J.H. Kim a, S.M. You a, Stephen U.S. Choi, 2004, Evaporative spray cooling of plain and microporous coated surfaces, International Journal of Heat and Mass Transfer, Vol. 47 pp. 3307–3315.

[7] S. Ujereh, T. Fisher, I. Mudawar, 2007, Int. J. Heat Mass Transfer, Vol. 50, pp. 4023–4038.

[8] Khanikar V., Mudawar I., Fisher T., 2009, International Journal of Heat and Mass Transfer, Vol. 52, pp. 3805-3817.